Sensors and Materials, Vol. 34, No. 2 (2022) 757–764
MYU Tokyo

S & M 2850

Radiophotoluminescence Imaging Reader for Passive Dosimetry

Hidehito Nanto,[1,2*] Go Okada,[1] Kazuki Hirasawa,[1]
Yasuhiro Koguchi,[2] Wakako Shinozaki,[2] Satoshi Ueno,[2]
Yuka Yanagida,[2] Francesco d'Errico,[3] and Takayoshi Yamamoto[2]

[1]Co-creative Research Center of Industrial Science and Technology, Kanazawa Institute of Technology, Hakusan, Ishikawa 924-0838, Japan
[2]Oarai Research Center, Chiyoda Technol Corporation, Oarai, Ibaraki 311-1313, Japan
[3]Department of Therapeutic Radiology, Yale University, New Haven 06510, U.S.A.

(Received October 12, 2021; accepted October 28, 2021)

Keywords: RPL, OSL, $CaSO_4$:Sm, X-ray imaging system, radiation measurement, phosphors, IP

In this study, we constructed an image reader system for two-dimensional radiation dosimetry based on radiophotoluminescence (RPL). The reader system mainly consists of a Peltier-cooled CMOS camera and an LED excitation source, as well as control units, and it offers an arbitrary excitation wavelength (e.g., 365, 405, 460, 530, and 630 nm) and a wide spectral detection range (200–1000 nm) to be used for a wide range of prototype image detectors having different spectral features. Using the developed system, we were able to successfully obtain X-ray projection images recorded on a commercial RPL detector [Ag-doped phosphate glass (Ag-PG) plate] as well as custom-made prototypes of flexible imaging plates (IPs). Furthermore, the reader system is applicable not only for RPL imaging but also for conventional optically stimulated luminescence (OSL) imaging, which was demonstrated by using a commercial IP for medical diagnosis.

1. Introduction

Radiophotoluminescence (RPL)[(1)] is a phenomenon in which luminescent centers are generated in a phosphor material through interaction with ionizing radiation. The number of luminescent centers produced is proportional to the integrated radiation dose and can generally be read as photoluminescence (PL) intensity. Currently, it is widely used in personal dosimetry for daily dose control.[(1,2)]

In a successful RPL material, the generated center is so stable that it is not affected by ambient environmental conditions such as light and temperature, as well as the excitation light during a readout. These properties allow a highly reliable dose measurement, particularly because it allows a signal readout multiple times, which effectively reduces statistical measurement uncertainties and is a distinct advantage over other related techniques using, for example, thermally stimulated luminescence (TSL),[(3–5)] optically stimulated luminescence (OSL),[(6)] and scintillation.[(7)]

*Corresponding author: e-mail: hnanto@neptune.kanazawa-it.ac.jp
https://doi.org/10.18494/SAM3686

ISSN 0914-4935
https://myukk.org/

Examples of existing phosphor materials that exhibit RPL are Ag-doped phosphate glass (Ag-PG),[8–10] C and Mg codoped aluminum oxide (Al_2O_3:C,Mg),[11,12] lithium fluoride (LiF),[13,14] and Sm-doped inorganic compound phosphors such as $SrBPO_5$,[15] $LiCaAlF_6$,[16] KBr,[17] CsBr,[18] MgF_2,[19] CaF_2,[20] $BaAlBO_3F_2$,[21] and $AESO_4$ (AE = Ca, Sr, Ba).[22] However, all of them are bulk solid phosphor materials and are not suitable for continuous dose distribution measurement (e.g., protective clothing and gloves) in curved areas. Given this background, we have been developing flexible dosimeters made of powdered RPL materials dispersed in resin.[23,24] In this paper, we report on the construction and evaluation of a two-dimensional imaging system using the RPL phenomenon for ionizing radiation, which is simple and inexpensive.

2. Materials and Methods

2.1 System configuration of image reader

Figure 1 shows the constructed reader system. Figure 1(a) reveals the appearance and Fig. 1(b) shows the system configuration. The system consists of a Peltier-cooled CMOS camera (2048 × 2048 pixels; CS-66UV, BITRAN Corp.), an objective lens (UV2528B, Universe Optical Industries Co., Ltd.), an optical filter [specs vary depending on the imaging plate (IP)], an LED disk (self-made), a dark box (self-made), a power supply (P4K36-1, Matsusada Precision Inc.), a

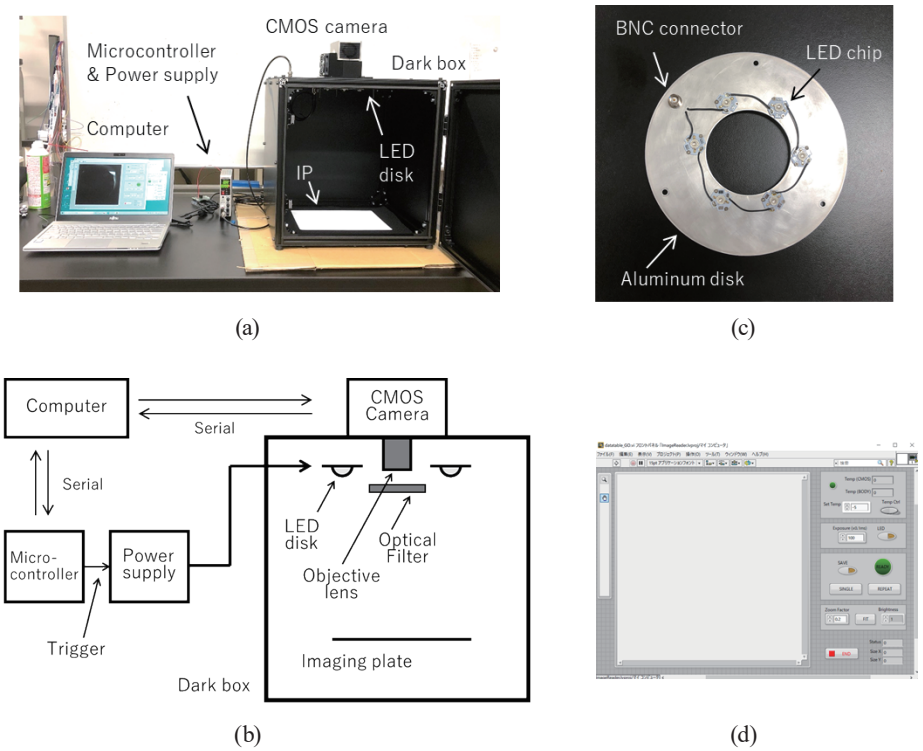

Fig. 1. (Color online) Image reader system. (a) Appearance, (b) system configuration, (c) LED array disk, and (d) control program.

microcontroller (Arduino UNO R3, Arduino), and a computer. Following a command from the computer, the microcontroller triggers the power supply to switch on/off the LED disk array, which optically excites/stimulates the IP. The LED disk array is shown in Fig. 1(c), in which several LED chips are distributed on an aluminum disk to ensure a uniform illumination of the IP. The luminescence pattern from the IP is viewed using the camera through the optical filter, and the image data are sent to the computer for recording. The wavelength of the LED array disk covers 365, 405, 460, 530, and 630 nm, in which the wavelength is selected by replacing the disk and/or by plugging the power cable to an appropriate connector. The full-width at half-maximum of the LED spectrum is typically ~5 nm. The spectral detection range of the camera is approximately 200–1000 nm, and the field of view is approximately 40 cm × 40 cm. The image acquisition can be operated using the original program coded by LabVIEW, as illustrated in Fig. 1(d).

2.2 Materials and characterization

The RPL materials used for the IPs in this study are Ag-PG and Sm-doped $CaSO_4$ ceramic powder (Sm-CSP). Ag-PG was manufactured by AGC Techno Glass Co., Ltd., whereas Sm-CSP was self-made via a solid-state reaction. The preparation method can be found elsewhere[25] but briefly described below. The powder reagents of $CaSO_4 \cdot 0.5H_2O$ (99% and up; KOJUNDO Chemical Laboratory) and Sm_2O_3 (99.9%, Wako Pure Chemical Industries) were weighed to the molecular ratio of 99.9:0.1 and then homogeneously mixed using a mortar and pestle. The mixture was loaded in an Al_2O_3 crucible and then heated at 1200 °C for 4 h in air inside an electric furnace (ETSS-430, Yamada Denki).

The basic RPL properties of the RPL materials were characterized using the TSL/OSL/RPL Automated and Integrated Measurement System (TORAIMS).[26] Here, the radiation source used was an X-ray tube (W anode, Be window, 40 kV) in which the tube current was controlled between 0.12 and 1.2 mA to vary the dose rate between 0.83 and 8.33 mGy/s. The delivery dose was controlled by changing the dose rate and irradiation time. For the measurement of the RPL signal, the material sample was excited by 340 nm light provided by a Xe arc lamp (LAX-C100, Asahi Spectra) and a band-pass optical filter (XRR0340, Asahi Spectra), and the luminescence spectrum was measured using a fiber-coupled multichannel spectrometer (QEPro, Ocean Optics).

3. Results and Discussion

Figure 2 shows X-ray images of the inside of an integrated circuit (IC) visualized with X-rays utilizing the RPL of Ag-PG phosphors. It can be seen that the inside of the IC is clearly visible. The orange emission from the outside of the IC, which is not shielded by the IC, is RPL from Ag-PG. Figure 2(b) shows an image acquired by using the reader system developed in this study. From the figure (arrowhead), we can see that the bonding wire goes between the lead electrode of the IC and the chip door at the center. Since the diameter of the bonding wire is usually about 25 μm, it can be seen that the spatial resolution is equal to or higher than that of a bonding wire.

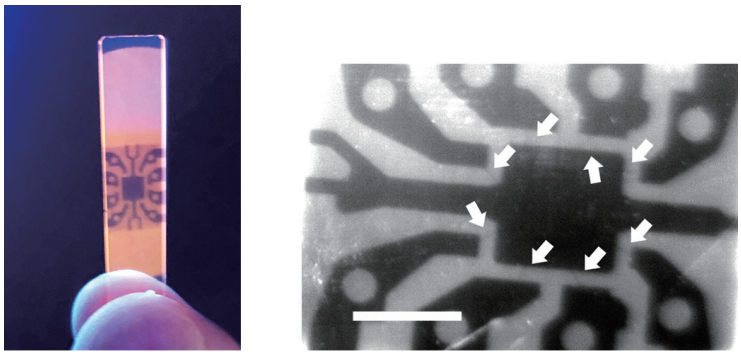

(a) (b)

Fig. 2. (Color online) X-ray images of an IC chip recorded on Ag-PG. (a) Appearance under 365 nm excitation and (b) image acquired by using the reader developed in this study (scale bar = 2 mm).

The two-dimensional RPL intensity distribution was read by a CMOS camera using 365 nm excitation light through a 400 nm cut filter. X-ray irradiation was performed using an X-ray tube (non-micro-focus, W target, 40 kV) at approximately 3 Gy.

Figure 3 shows the PL spectra from Sm-CSP phosphor samples irradiated with X-rays (250, 500, and 1000 mGy). The samples show sharp emission features peaking at 560, 595, 643, and 705 nm, regardless of radiation dose. The origin of these emission lines is attributed to the parity-forbidden 4f–4f transitions of Sm^{3+}. After the irradiation, however, the spectral features change considerably. In addition to Sm^{3+} emissions, a very strong broad emission band peaking at 630 nm as well as multiple sharp lines across the 680–820 nm range appear in the spectrum. From the spectral features, the former emission is assigned to the 5d–4f transitions of Sm^{2+}, whereas the latter is attributed to the 4f–4f transitions of Sm^{2+}. From these observations, we conclude that the Sm^{2+} ion has been generated by irradiating Sm-CSP with X-rays.[25]

To obtain two-dimensional X-ray images using Sm-CSP phosphor powder, we fabricated two different types of prototype RPL-IPs shown in Fig. 4. The first type illustrated in Fig. 4(a) is a flexible film type, in which Sm-CSP is embedded in a polyvinyl alcohol (PVA) matrix, whereas the other type shown in Fig. 4(b) was fabricated by coating Sm-CSP on a plastic substrate. For the PVA-based RPL-IP, a problem remains on how to disperse the phosphor powder uniformly. On the other hand, Sm-CSP was coated fairly uniformly for the flexible plate-type RPL-IP. Therefore, we used the latter type for imaging demonstration in this study. Figure 4(c) shows an X-ray image of a paper clip acquired by using the flexible plate-type RPL-IP. The X-ray dose was 10 Gy, and the excitation LED wavelength was 365 nm. As can be seen from the figure, the image of the paper clip is clearly projected. As future work, we will continue to improve and develop further a sheet RPL-IP by aiming to realize a sheet dosimeter with uniformly dispersed or coated phosphors of A4 size.

In addition, as a supplemental feature of the image reader system constructed, X-ray imaging was demonstrated by using a commercial OSL-IP (BAS-MS, Fuji Photo Film Co., Ltd.) in which a Eu-doped BaFBr phosphor is used as a sensing element.[27] This IP is based on the OSL

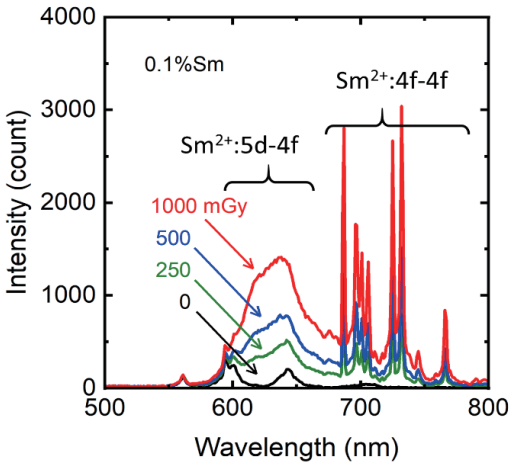

Fig. 3. (Color online) X-ray dose (0, 250, 500, and 1000 mGy) dependence of PL spectra of Sm-CSP.

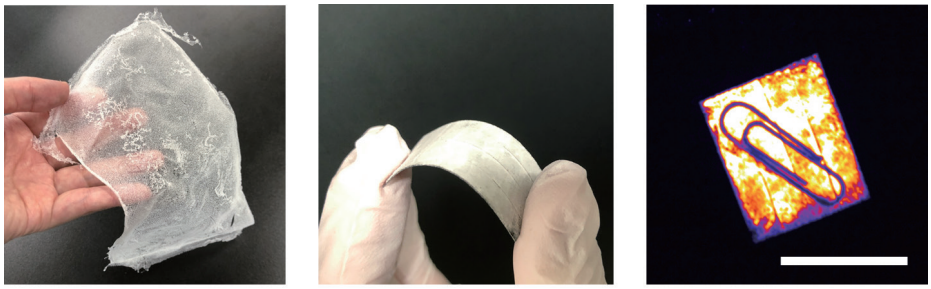

(a) (b) (c)

Fig. 4. (Color online) Prototypes of flexible RPL-IP and demonstration of X-ray imaging. (a) Flexible film type in which Sm-CSP is embedded in a PVA matrix. (b) Flexible plate type where a plastic plate is coated with Sm-CSP. (c) X-ray image of a paper clip acquired by using the plate-type RPL-IP (scale bar = 2 cm).

phenomenon and is now widely used as an X-ray imaging medium for medical and dental diagnoses. The OSL phenomenon[28] is also an attractive luminescence phenomenon used in radiation measurements, similarly to the RPL phenomenon. It is observed in a phosphor where incident radiation energy is stored in the form of trapping charges generated by radiation. The trapped charges can be reactivated by optical stimulation, and then they recombine at a luminescent center to emit light. The emitted light intensity is proportional to the number of trapped charges, which is proportional to the incident radiation dose; therefore, the OSL allows us to indirectly measure the radiation dose in the form of light intensity.

Figure 5 shows X-ray images of (a) a computer mouse, (b) pocket tools in a plastic case, (c) a credit card, and (d) a blackthroat seaperch (*nodoguro*) caught off the coast of the Sea of Japan in Ishikawa Prefecture. The LED wavelength was 630 nm. All of the X-ray images are clear and crisp, indicating that the X-ray imaging system developed in this study is also applicable for imaging using the OSL-IP.

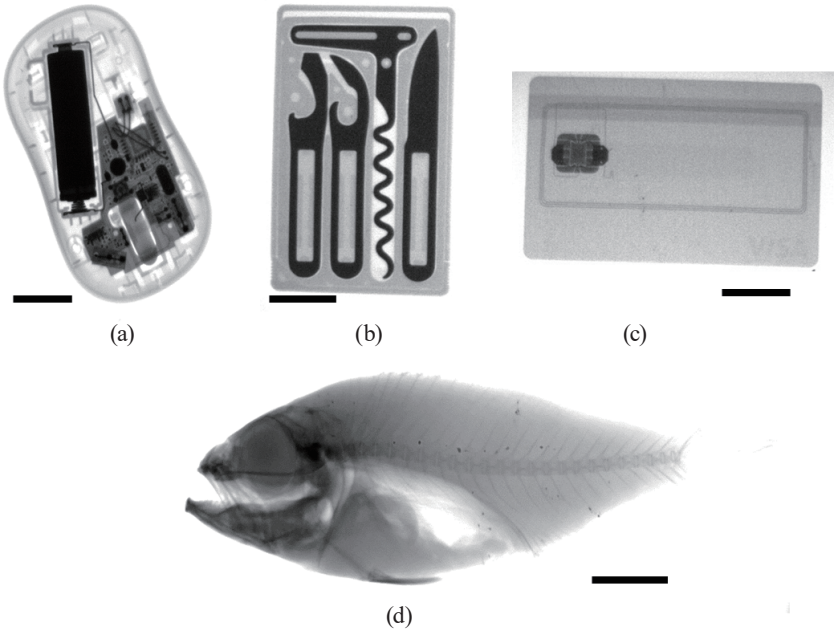

Fig. 5. (Color online) X-ray images of (a) a computer mouse, (b) pocket tools in a plastic case, (c) a credit card, and (d) a blackthroat seaperch (*nodoguro*) caught off the coast of the Sea of Japan in Ishikawa Prefecture. All the images were acquired by using an OSL-IP (BAS-MS, Fuji Photo Film Co., Ltd.) and the image reader system developed in this study (scale bar = 2 cm).

We previously reported on the measurement of a two-dimensional radiation dose distribution using the RPL phenomenon of Ag-PG phosphor sheets and its readout system.[24] To measure a two-dimensional RPL image using this system, the readout system was mainly composed of an x-y stage (A4 size), a UV LED, and a laptop computer. The image is monitored by scanning the focused UV light on the irradiated sheet-type Ag-PG dosimeter. Therefore, this X-ray image reading system has the following problems. (1) The readout light source is fixed, so it cannot be used for radiation-induced phosphors other than Ag-PG phosphors. (2) It takes about three hours to read out an image of A4 size, which is a long time to read an image. (3) The system is large and the fabrication cost is also high. On the other hand, the image reader system developed in this study uses a CMOS camera for image acquisition and multiple excitation light sources for reading out the X-ray image, which eliminates all the above problems and makes the system very easy to use. The resolution of the image obtained is the same or higher than that of the image obtained using the previous system.

4. Conclusion

We constructed a two-dimensional RPL image reader system for passive dosimetry and then evaluated its performance. As a result, by imaging with Ag-PG, we could obtain a high resolution with which the writing of the IC could be transmitted clearly by using the constructed system. Furthermore, we fabricated a flexible Sm-CSP phosphor sheet, which was found to be effective

for measuring two-dimensional X-ray images, i.e., a two-dimensional radiation dose distribution.

Acknowledgments

This work was financially supported by a Grant-in-Aid for Challenge Research (Exploratory) (19K22158) and a Grant-in-Aid for Early-Carrier Scientists (20K15207) from the Ministry of Education, Culture, Sports, Science and Technology of the Japanese government (MEXT), Japan, as well as the Nuclear Power Safety Technology Research Center, Chubu Electric Power Co., Inc. The Cooperative Research Project of the Research Institute of Electronics, Shizuoka University is also acknowledged. Furthermore, we would also like to thank Mrs. Tokiko Nanto for obtaining the blackthroat seaperch (*nodoguro*).

References

1 G. Okada: J. Chem. Soc. Jpn. **129** (2021) 21056. https://doi.org/10.18494/SAM.2017.1624
2 G. Okada, T. Yanagida, S. Kasap, and H. Nanto: Kinzoku **89** (2019) 38 (in Japanese).
3 S. W. S. McKeever: Thermoluminescence of Solids (Cambridge University Press, 1985).
4 K. Shinsho, K. Otsubo, Y. Koba, K. Matsumoto, and H. Ushiba: Sens. Mater. **28** (2016) 917. https://myukk.org/SM2017/sm_pdf/SM1252.pdf
5 R. Oh, S. Yanagisawa, H. Tanaka, T. Takata, G. Wakabayashi, M. Tanaka, N. Sugioka, Y. Koba, and K. Shinsho: Sens. Mater. **33** (2021) 2129. https://myukk.org/SM2017/sm_pdf/SM2599.pdf
6 S. W. S. McKeever: Radiat. Meas. **46** (2011) 1336. https://doi.org/10.1016/j.radmeas.2011.02.016
7 T. Yanagida: Proc. Jpn. Acad. Ser. B **94** (2018) 75. https://doi.org/10.2183/pjab.94.007
8 R. Yokota and H. Imagawa: J. Phys. Soc. Jpn. **23** (1966) 1038. https://doi.org/10.1143/JPSJ.23.1038
9 T. Yamamoto, Y. Yanagida-Miyamoto, T. Iida, and H. Nanto: Radiat. Meas. **136** (2020) 106363. https://doi.org/10.1016/j.radmeas.2020.106363
10 T. Kurobori, W. Zheng, Y. Miyamoto, H. Nanto, and T. Yamamoto: Opt. Mater. **32** (2010) 1231. https://doi.org/10.1016/j.optmat.2010.04.004
11 M. S. Akselrod and A. E. Akselrod: Radiat. Prot. Dosimetry **119** (2006) 218. https://doi.org/10.1093/rpd/nci663
12 M. Akselrod and J. Kouwenberg: Radiat. Meas. **117** (2018) 35. https://doi.org/10.1093/rpd/nci663
13 M. Levita, T. Schlesinger, and S. S. Friedland: IEEE Trans. Nucl. Sci. **23** (1976) 667. https://doi.org/10.1109/TNS.1976.4328325
14 A. Mrozik, P. Bilski, B. Marczewska, B. Obryk, K. Hodyr, and W. Gieszczyk: Radiat. Meas. **71** (2014) 31. https://doi.org/10.1016/j.radmeas.2014.05.013
15 G. Belev, G. Okada, D. Tonchev, C. Koughia, C. Varoy, A. Edgar, T. Wysokinski, D. Chapman, and S. Kasap: Phys. Status Solidi **8** (2011) 2822. https://doi.org/10.1002/pssc.201084103
16 G. Okada, N. Kawaguchi, S. Kasap, H. Nanto, and T. Yanagida: Radiat. Meas. **132** (2020) 106251. https://doi.org/10.1016/j.radmeas.2020.106251
17 G. Okada, Y. Fujimoto, H. Tanaka, S. Kasap, and T. Yanagida: J. Mater. Sci. Mater. Electron. **28** (2017) 15980. https://doi.org/10.1007/s10854-017-7496-z
18 G. Okada, Y. Fujimoto, H. Tanaka, S. Kasap, and T. Yanagida: J. Rare Earths **34** (2016) 769. https://doi.org/10.1016/S1002-0721(16)60092-3
19 G. Okada, F. Nakamura, N. Kawano, N. Kawaguchi, S. Kasap, and T. Yanagida: Nucl. Instrum. Methods Phys. Res., Sect. B **435** (2018) 268. https://doi.org/10.1016/j.nimb.2018.01.032
20 G. Okada, J. Ueda, S. Tanabe, G. Belev, T. Wysokinski, D. Chapman, D. Tonchev, and S. Kasap: J. Am. Ceram. Soc. **97** (2014) 2147. https://doi.org/10.1111/jace.12938
21 G. Okada, K. Shinozaki, T. Komatsu, S. Kasap, and T. Yanagida: Radiat. Meas. **106** (2017) 73. https://doi.org/10.1016/j.radmeas.2016.12.006
22 G. Okada, K. Hirasawa, E. Kusano, T. Yanagida, and H. Nanto: Nucl. Instrum. Methods Phys. Res., Sect. B **466** (2020) 56. https://doi.org/10.1016/j.nimb.2020.01.020
23 F. d'Errico, L. Abegao, S. O. Souza, A. Chierici, L. Lazzeri, M. Puccini, S. Vitolo, Y. Miyamoto, H. Nanto, and T. Yamamoto: Radiat. Meas. **137** (2020) 106423. https://doi.org/10.1016/j.radmeas.2020.106423

24 H. Nanto, Y. Yanagida, M. Sugiyama, Y. Koguchi, Y. Ihara, K. Shimizu, T. Ikeguchi, K. Hirasawa, Y. Takei, and T. Yamamoto: Sens. Mater. **29** (2017) 1439. https://doi.org/10.18494/SAM.2017.1624
25 G. Okada, W. Shinosaki, S. Ueno, Y. Koguchi, K. Hirasawa, F d'Errico, T. Yanagida, S. Kasap, and H. Nanto: Jpn. J. Appl. Phys. (2021). https://doi.org/10.35848/1347-4065/aclab2
26 G. Okda, K. Hirasawa, T. Yanagida, and H. Nanto: Sens. Mater. **33** (2021) 2117. https://doi.org/10.18494/SAM.2021.3327
27 Y. Amemiya and J. Miyahara: Nature **336** (1988) 89. https://doi.org/10.1038/336089a0
28 H. Nanto: Sens. Mater. **30** (2018) 327. https://doi.org/10.18494/SAM.2018.1803